

# Geophysical Research Letters

## RESEARCH LETTER

10.1029/2019GL084613

### Key Points:

- We predict fracture growth in four X-ray tomography experiments using the machine learning method of logistic regression
- The best predictors of growth are the fracture size, length, aperture, and orientation and fracture network clustering
- Growing fractures are smaller in volume, shorter, thinner, more obliquely dipping from  $\sigma_1$ , and more clustered than closing fractures

### Supporting Information:

- Supporting Information S1

### Correspondence to:

J. McBeck,  
j.a.mcbeck@geo.uio.no

### Citation:

McBeck, J., Kandula, N., Aiken, J. M., Cordonnier, B., & Renard, F. (2019). Isolating the factors that govern fracture development in rocks throughout dynamic in situ X-ray tomography experiments. *Geophysical Research Letters*, 46, 11,127–11,135. <https://doi.org/10.1029/2019GL084613>

Received 20 JUL 2019

Accepted 25 SEP 2019

Accepted article online 15 OCT 2019

Published online 29 OCT 2019

## Isolating the Factors That Govern Fracture Development in Rocks Throughout Dynamic In Situ X-Ray Tomography Experiments

Jessica McBeck<sup>1</sup> , Neelima Kandula<sup>1</sup> , John M. Aiken<sup>2,3</sup>, Benoît Cordonnier<sup>1,4</sup>, and François Renard<sup>1,5</sup> 

<sup>1</sup>Physics of Geological Processes, The Njord Centre, Department of Geosciences, University of Oslo, Oslo, Norway, <sup>2</sup>Center for Computing in Science Education, Department of Physics, University of Oslo, Oslo, Norway, <sup>3</sup>Department of Physics and Astronomy, Michigan State University, East Lansing, MI, USA, <sup>4</sup>Beamline ID19, The European Synchrotron and Radiation Facility, Grenoble, France, <sup>5</sup>University Grenoble Alpes, University Savoie Mont Blanc, CNRS, IRD, IFSTTAR, ISTerre, Grenoble, France

**Abstract** Centuries of work have highlighted the importance of several characteristics on fracture propagation. However, the relative importance of each characteristic on the likelihood of propagation remains elusive. We rank this importance by performing dynamic X-ray microtomography experiments that provide unique access to characteristics of evolving fracture networks as rocks are triaxially compressed toward failure. We employed a machine learning technique based on logistic regression analysis to predict whether or not a fracture grows from 14 fracture geometry and network characteristics identified throughout four experiments on crystalline rocks in which thousands of fractures propagated. The characteristics that best predict fracture growth are the length, thickness, volume, and orientation of fractures with respect to the external stress field and the distance to the closest neighboring fracture. Growing fractures tend to be more clustered, shorter, thinner, volumetrically smaller, and dipping closer to 30–60° from the maximum compression direction than closing fractures.

**Plain Language Summary** What controls fracture growth in rocks? Previous work highlights the importance of many characteristics on the likelihood of fracture growth but has not ranked the importance of these characteristics. We use triaxial compression experiments of rocks and machine learning to predict fracture growth using measures of the fracture network clustering and fracture size, shape, and orientation. The characteristics that are the best predictors of fracture growth are the fracture length, thickness, volume, and orientation and distance to the nearest fracture. Fractures that grow (increase in volume) during each increase in differential stress are shorter, thinner, smaller in volume, and more clustered than fractures that close (decrease in volume).

## 1. Introduction

Predicting when and how faults propagate and interact is a fundamental challenge in geosciences. Over the past century, analyses have isolated the importance of several factors on fracture development, including the spatial distribution and orientation of fractures with respect to an external stress field, the proximity to pre-existing weaknesses and neighboring fractures, and the length, aperture, and shape of fractures (e.g., Anderson, 1942; Dahlen, 1984; Griffith, 1921; Hubbert, 1951; Irwin, 1957; Raju & Newman, 1979; Rybicki & Kanninen, 1977; Sih, 1974). However, such analyses were not able to compare the relative importance of these factors on the likelihood of fracture propagation to each other. This gap in knowledge causes scientists to categorize a multitude of properties of fault networks in order to predict fault interaction.

In situ dynamic X-ray microtomography experiments reveal precise details of fracture growth and coalescence within crustal rocks under triaxial compression (e.g., Renard et al., 2017, 2018). Time series of 3-D X-ray attenuation fields, that is, tomograms, captured after loading steps during triaxial compression experiments reveal the geometries of individual opening fractures within evolving fracture networks as the rocks are driven toward macroscopic failure (Figure 1). Algorithms that track each identified fracture indicate how individual fractures interact and grow within the network (Kandula et al., 2019). These experiments and postprocessing techniques provide unprecedented access to factors that control microfracture

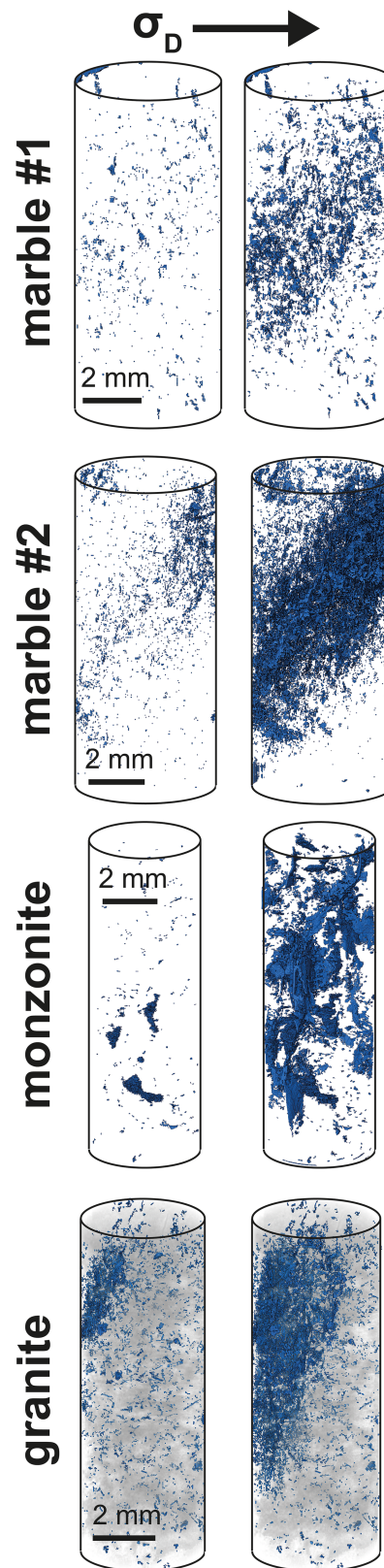


**Figure 1.** Fracture development within in situ X-ray tomography triaxial compression experiments. Snapshots of fracture networks (blue) at (left) lower and (right) higher differential stresses during four analyzed experiments on marble, monzonite, and granite. With increasing differential stress, some fractures lengthen and open, while others close, and the fracture network becomes increasingly clustered.

development to varying degrees. Machine learning techniques enable quantifying the importance of each factor on fracture development. In recent years, geoscientists have used machine learning to understand and predict earthquakes in the lab and the field (e.g., Asencio-Cortés et al., 2017; Asim et al., 2017; Bergen et al., 2019; Reyes et al., 2013; Rouet-Leduc et al., 2017). However, none of these analyses have yet attempted to predict the likelihood of fracture propagation through intact rock, nor have they rank the importance of recognized controls on fracture development.

Here we aim to determine the importance of a suite of fracture characteristics on the likelihood of fracture propagation (Figure S1 in the supporting information). To achieve this goal, we built and trained logistic regression models (e.g., Cox, 1958; Hosmer et al., 2013) that predict whether an individual fracture will grow using measures of its size (i.e., length, aperture, and volume), shape (i.e., anisotropy and elongation), orientation, and position within the fracture network (i.e., clustering) (Figure S2). Then we used recursive feature elimination (e.g., Guyon et al., 2002) to identify the fracture characteristics that are the best predictors of propagation (Figure S1). Finally, we tracked the statistical properties of these predictors from the onset of loading until macroscopic failure to pinpoint the quantities that characterize fractures that are growing (gaining volume) and those that are closing (losing volume). Determining the criteria that exert the greatest impact on fracture network evolution may improve seismic hazard assessments of natural fault systems. Rather than categorizing many and perhaps insignificant fault network properties, more cost- and time-efficient field studies could focus on the properties that exert the greatest influence on fracture development.

## 2. Methods

### 2.1. Experimental Design and Fracture Tracking

We analyze results from four rock deformation experiments that include rock types representative of low-porosity crystalline rocks within the continental crust: two on Carrara marble, one on monzonite, and one on Westerly granite (Table S1). In each experiment, we increased the differential stress,  $\sigma_D$ , applied to a 1-cm-tall and 0.5-cm-wide rock core, with  $\sigma_1$  parallel to the axis of the core, while the confining stress,  $\sigma_2 = \sigma_3$ , was held constant until the core macroscopically failed. Under constant confining stress, we increased the axial stress in steps of 0.5–5 MPa, with smaller steps closer to failure, and acquired a time series of X-ray tomograms at a resolution of 6.5  $\mu\text{m}$  per voxel edge, at beamline ID19 at the European Synchrotron Radiation Facility using the Hades deformation apparatus (Renard et al., 2016; Table S1).

We segmented the tomograms into fractures and intact rock using a nonlocal mean filter and several additional image processing techniques developed by Renard et al. (2018). Tracking an individual fracture from the moment when it appears to when it closes or merges with another fracture, or when the rock macroscopically fails, is a nontrivial problem. As the core shortens axially and expands radially, fractures may translate in space in the absence of propagation, opening or closure. Kandula et al. (2019) developed algorithms to solve this nontrivial problem and track individual fractures (labeled with unique identifiers) throughout microtomography experiments. We employed this approach to track fractures here and followed the evolution of thousands of fractures toward failure in each sample.

### 2.2. Feature Extraction From Fractures and Fracture Networks

In each experiment, we tracked the evolution of every fracture using the voxel locations of the fractures identified with the tracking algorithm (Table S1). For each fracture, we calculated 14 measures that quantify the geometry, size, and orientation of each fracture or its proximity to other fractures within the fracture network. We selected these measures because previous formulations of linear elastic fracture mechanics predict the likelihood of fracture growth using these characteristics (e.g., Anderson, 1942; Dahlen, 1984; Griffith, 1921; Hubbert, 1951; Irwin, 1957; Raju & Newman, 1979; Rybicki & Kanninen, 1977; Sih, 1974).

We quantify the proximity of each fracture to the others in the network by calculating the minimum, mean, and median distances from the centroid of each fracture to all the other fracture centroids in the network. We also calculated these values for each fracture using the 25th percentile of other fractures with centroids nearest to its centroid. Analyzing these two sets of distance measures indicates whether the local or global fracture network is a better predictor of fracture development.

To characterize the geometry of each fracture, we calculated the covariance matrix of the set of voxels that represent each fracture and the corresponding eigenvectors and eigenvalues. The covariance matrix is

equivalent to the inertial moment tensor if each voxel corresponds to a point mass of unity located at its centroid. The eigenvectors define the orientations relative to a Cartesian coordinate system. The eigenvalues define the size and shape of each fracture (Figure S2). The largest and smallest eigenvalues are not strictly equal to, but represent, the length and aperture of the fractures. From the eigenvalues, we calculated the anisotropy (1 minus the minimum eigenvalue divided by the maximum eigenvalue) and elongation (1 minus the intermediate eigenvalue divided by the maximum eigenvalue) of each fracture. We also included the volume of each fracture as a model feature. To determine whether or not a fracture grows or closes from one scan to the next (after a stress step increase), we calculated the change in volume of the fracture. This binary classification of whether a fracture grows or closes is the outcome that we trained the models to predict.

One may expect that boundary effects due to friction between the pistons and core interfaces could influence the location of the population of closing and growing fractures. To assess this influence, we examined the spatial distribution of these populations of fractures relative to the piston positions at the top and bottom of the sample (Figure S3). The distributions of vertical positions of the growing and closing fractures are similar to each other in each experiment. Closing fractures are not preferentially located near the pistons, as could be expected. Boundary effects do not appear to influence whether fractures grow or close.

### 2.3. Logistic Regression Models

We used one of the most common linear classification methods to predict the binary outcome of fracture growth or closure: logistic regression (e.g., Cox, 1958). Logistic regression is a statistical approach that uses a logistic function to produce a binary (true/false) prediction from input data (i.e., features). We choose to develop logistic regression models because we wished to predict the binary outcome of whether a fracture grew or not. In addition, logistic regression provides output that is relatively easy to interpret because the model assumes a linear trend between model features (e.g., Hosmer et al., 2013).

In this study, we developed individual logistic regression models for each experiment, and 50 individual models on randomly selected subsets of the data for each experiment. The number of identified growing fractures exceeds the number of closing fractures in each experiment. To account for this imbalance in determining the model success, and to aid the robustness of the results, we built 50 individual logistic regression models from randomly selected subsets of the data of each experiment. We used all of the fractures identified as closing fractures, counted the number of these fractures, and then randomly selected the same number of growing fractures. Then we trained each model using 80% of the fractures identified at each stress step and tested the success of the model with the remaining 20% of the data in each of the experiments. The training and testing data sets were entirely separate in that we only included data from a particular fracture at a given stress step in either the training or testing data sets. We performed a cross-validated grid search over the parameters of the models to find the best set of parameters. We employed the Python Scikit-learn library to build, train, and test these models (Pedregosa et al., 2011).

We used recursive feature elimination (Guyon et al., 2002) with threefold cross validation (RFECV) to identify the best explanatory, or predictive, features of the model. RFECV orders the features by coefficient magnitude (smallest to largest) and then removes the features one by one, refitting and scoring the model using a selected scoring metric. As features are removed, the scoring metric typically remains the same or decreases until the model has an acceptable minimum score. The remaining features represent the characteristics that are the best predictors of the outcomes of the model. Here we used the accuracy scoring metric for RFECV. Accuracy is defined as the number of true model predictions out of the number of total (true and false) predictions.

## 3. Results

### 3.1. Success of Logistic Regression Models

We developed and trained logistic regression models for the four experiments to predict whether a fracture grows or closes using 14 characteristics of each fracture. We assess the success of the models using the recall and precision scoring metrics. The recall reflects the positive predictive value, while the precision reflects the sensitivity (e.g., Müller & Guido, 2016). Higher scores indicate greater model success, with scores of 1



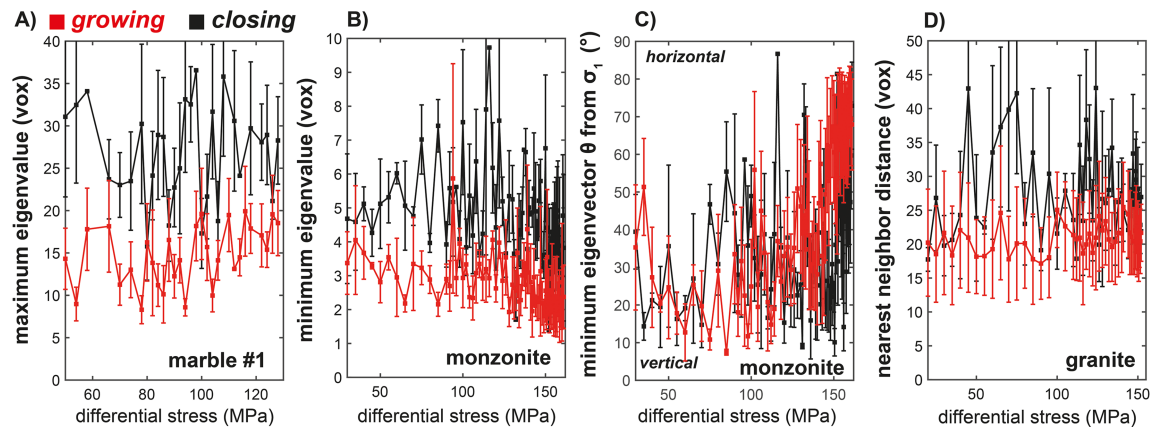


**Figure 2.** Evolution of controls on fracture growth. Recursive feature elimination highlights the best predictors of growth (Figure S6): the (a) maximum and (b) minimum eigenvalues of the fractures, (c) the orientation of the eigenvector with the minimum eigenvalue relative to  $\sigma_1$ , and (d) the nearest-neighbor distance from each fracture. Red and black lines and markers show the mean  $\pm$  one standard deviation of population of fractures that are growing and closing between subsequent stress steps. The lengths are in units of the edge length of the voxels of the tomograms (1 vox. = 6.5  $\mu\text{m}$ ).

indicating sets of perfect model predictions. We report the mean  $\pm$  one standard deviation of the scores produced by the 50 models for each experiment (Figure S4).

The recall and precision of the models increase as we remove fractures that are growing or closing by increasing percentages of their volume (i.e., data removal threshold; Figures S4 and S5). This increase in performance may arise from the segmentation procedure used to extract fractures. Segmentation may influence the model success if a fracture translates in space between scan acquisitions (and thus stress steps) but does not grow or close. This translation may produce apparent changes in the number of voxels included in the fracture (volume) due to differences in the intersection of the fracture with the predefined voxel grid of the scan. The increasing success of the models with increasing data removal threshold suggests that differences in fracture segmentation across subsequent tomograms may produce artificial changes in volume that do not reflect fracture propagation, opening or closing. Although this thresholding reduces the amount of data used to train and test the models, it improves the quality of the data and thus the models' success.

In the subsequent exploration of the importance of each characteristic on the predictions of the models, we focus on populations of fractures growing or closing by more than 50% of their volume in one stress step, from one scan to the next. For fractures growing or closing more than 50% of their volume, the recall and precision scores are 0.70–0.80 (Figure S4). Consequently, this threshold produces models with acceptably high success rates and includes a larger population of growing and closing fractures than higher thresholds.

### 3.2. Importance of Fracture Characteristics on Growth

To extract the fracture network characteristics that are the best predictors of fracture development, we employed recursive feature elimination with cross validation (RFECV). This technique ranks the importance of each feature on the model predictions, indicating the best explanatory, or most predictive, features (Guyon et al., 2002). We used recursive feature elimination to select the features that are the best predictors of fracture growth in the 50 independent logistic regression models of the four experiments, producing 200 rankings of the importance of each feature.

The most important features selected by recursive feature elimination in the 50 models of the four experiments include characteristics of the geometry of each fracture, its orientation with respect to the applied stress, and the clustering of the local and global fracture network (Figure S6). We identify the most important features across all the experiments as those that produce  $>75\%$  of the maximum cumulative importance. These features include the volume of the fracture; the largest, intermediate, and minimum eigenvalues; the orientation of the eigenvector with the minimum eigenvalue; and the minimum distance between fracture centroids.

We now focus on the differences between these characteristics of the population of fractures that are growing and closing. Figure 2a shows the mean  $\pm$  one standard deviation of the maximum and minimum

eigenvalues, indicative of the fracture length and aperture, of the growing and closing fractures in the marble and monzonite experiments. The maximum eigenvalues of closing fractures are greater than the maximum eigenvalue of growing fractures in these experiments (Figure 2a). In contrast to the expectations from stress intensity formulations, shorter fractures are more likely to grow than are longer fractures. Similarly, the minimum eigenvalues of closing fractures are larger than the minimum eigenvalues of growing fractures (Figure 2b). Thinner fractures are more likely to grow than are thicker fractures. Consistent with these trends, closing fractures tend to have higher volumes and larger intermediate eigenvalues than do growing fractures.

Figure 2c shows the mean  $\pm$  one standard deviation of the orientation of the eigenvector with the minimum eigenvalue of the growing and closing fractures in the monzonite experiment. This orientation is the orientation of smallest dimension of the fracture relative to the principal stress directions. Both closing and growing fractures have similar ranges of this orientation until the rock begins to approach failure. However, above a differential stress of 125 MPa, the population of closing fractures tend to have these eigenvectors near to parallel to the maximum compressive stress,  $\sigma_1$  (Figure 2c). Growing fractures tend to have these eigenvectors at more oblique orientations relative to closing fractures, from  $30^\circ$  to  $80^\circ$  from  $\sigma_1$ .

Figure 2d shows the mean  $\pm$  one standard deviation of the nearest-neighbor distance between sets of growing and closing fractures in the granite experiment. The nearest-neighbor distances of growing fractures are smaller than the distances of closing fractures (Figure 2d). Fractures that grow near another fracture have a greater likelihood of propagation than do fractures that grow at greater distances from other fractures in the network.

## 4. Discussion

This analysis of four in situ triaxial compression dynamic microtomography experiments indicates that the characteristics that provide the most accurate predictions of fracture growth are the following: the volume and eigenvalues of the fracture (indicative of fracture length and aperture), the orientation of the eigenvector with the smallest eigenvalue (fracture orientation), and the nearest-neighbor distance between fracture centroids (fracture network clustering).

### 4.1. Fracture Network Clustering

The mean and median distances to nearby fractures (within the closest 25th percentile of the distances between fractures) are not strong predictors of fracture development, and neither are the mean and median distances to all of the identified fractures in the system (Figure S6). The only clustering measure that ranks highly in importance is the distance to the closest fracture. More clustered fractures, which are close to at least one other fracture, are more likely to propagate than are more dispersed fractures (Figure 2d).

This trend is consistent with field observations indicating that an earthquake that begins on one fault is more likely to trigger a seismic event on an adjacent fault if the faults are within a few kilometers of each other than if the faults are further apart (Wesnousky, 2006). Although earthquakes are primarily shear rupture events and the experimental fracture growth we detect must contain opening-mode deformation, the trends observed in earthquake triggering and experimental fracture growth are similar because both opening-mode and shear deformation perturb the local stress and strain field.

The elastic perturbation of the local stress and strain fields due to slip and opening allow fractures and faults to interact at some distance away from each other and not only when their segments comprise one continuous fault surface. This interaction causes nearby fault segments to produce cumulative along-strike slip distributions that match the slip distributions of individual faults, with approximately bell-shaped or elliptical distributions (e.g., Bürgmann et al., 1994). Similarly, the power law relationship observed in X-ray tomography experiments between the distance to macroscopic failure and fracture volume may arise from long-range elastic interactions between fractures in the network (Kandula et al., 2019).

Our results suggest that field analyses that aim to understand fracture development should focus on the nearest-neighbor distance between fractures. These analyses may not need to consider the position of the fracture within the larger fault network to provide robust predictions of fault development, but only the distance to the closest fault. This result may simplify the difficult task of selecting the appropriate system size

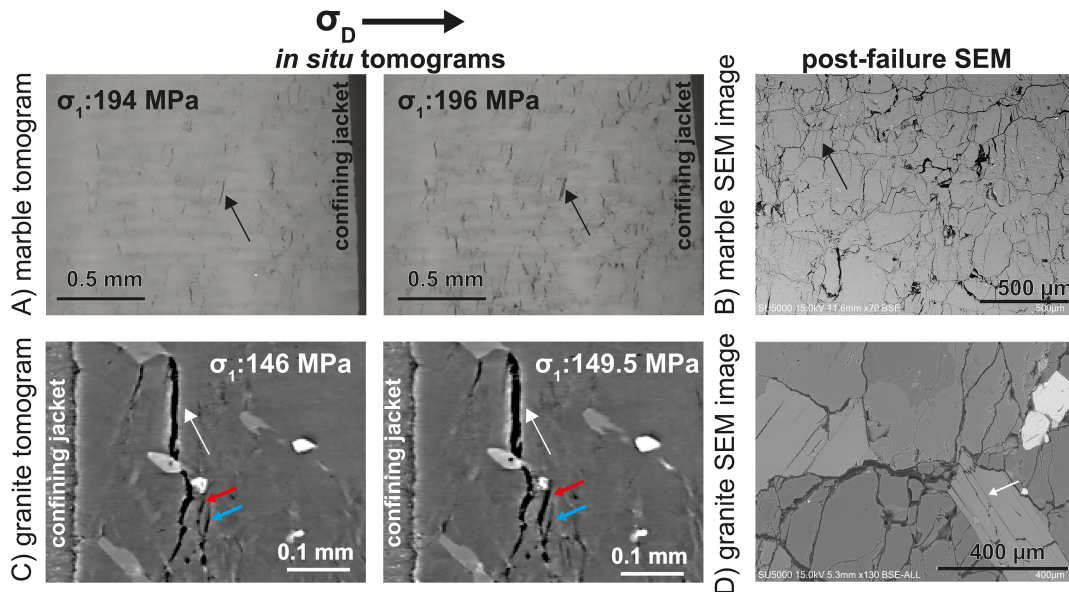


**Figure 3.** Influence of heterogeneities on fracture propagation. Two-dimensional slices of in situ X-ray tomograms of the (a) marble and (c) granite experiments, and scanning electron microscopy images of post-failure (b) marble and (d) granite cores recovered after experiments. (a, b) Black arrows indicate fractures pinned by grain boundaries. (c, d) White arrows indicate fractures impeded by minerals and grain boundaries. (c) Red arrow shows fracture that grows near to fracture that closes (blue arrow).

and thus population of faults to assess. However, differences between the observability of experimental fracture networks and crustal fault networks may limit the applicability of this finding.

Another key factor in this analysis is the appropriate length scale of faults to consider. Whereas we can detect all of the open fractures in the tomograms, field analyses must select the appropriate length scale of faults to consider when searching for nearest neighbors. Nominally intact crustal rock contains preexisting fractures surrounding plate boundary faults, so potential analyses of the nearest-neighbor distance between faults in the field must decide on the spatial scale of faults to include.

#### 4.2. Fracture Length

Our analysis shows that closing fractures tend to have greater maximum eigenvalues (length) than do growing fractures (Figure 2a). The stress intensity factor at a fracture tip indicates the likelihood of fracture

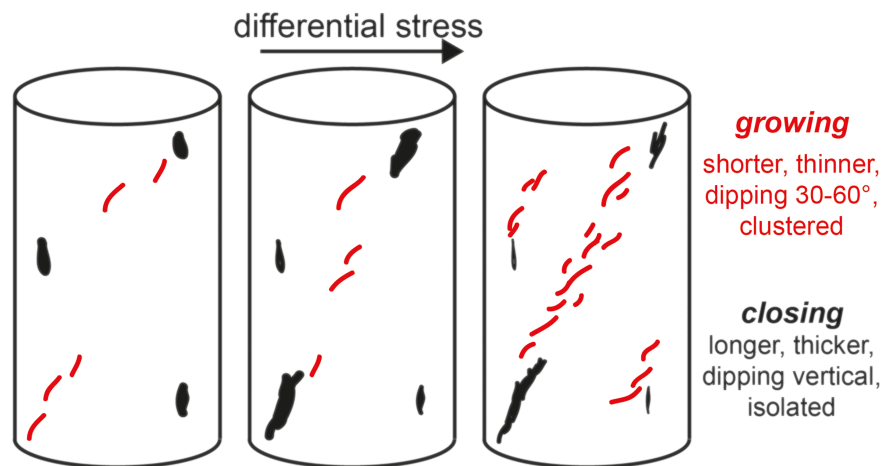


**Figure 4.** Characteristics of growing and closing fractures. Schematic illustration of characteristics of fractures that are growing (red) and closing (black) with increasing differential stress. Growing fractures tend to be shorter, thinner, more obliquely dipping to  $\sigma_1$ , and clustered than do closing fractures. Fractures may transition from growing to closing as fractures coalesce, forming thicker fractures that are less optimally oriented for slip. New fractures may nucleate and grow near closing fractures as closure amplifies local stress concentrations.

propagation using the length and shape of the fracture (e.g., Isida, 1971; Raju & Newman, 1979). Longer mode I fractures produce greater stress intensity factors, increasing the likelihood of propagation in the absence of changes in the external stress field. Our results conflict with the expectations of linear elastic fracture mechanics because the fractures do not develop in isolation in our experiments. As fractures propagate and coalesce, they modify the local stress field, producing and propagating into regions with varying magnitudes of normal and shear stress. Shorter fractures may have a higher likelihood of fracture propagation than do longer fractures because they tend to be more clustered than do longer fractures, as measured with the nearest-neighbor distance (Figure 2d).

The heterogeneous strength distribution of the rocks may also impact the observed trend of shorter fractures growing and longer fractures closing. Two-dimensional slices of tomograms and scanning electron microscope images show intragranular fractures that terminate at the edges of grain boundaries in the marble experiment (Figures 3a and 3b). These fractures likely exploit cleavage planes within the calcite grains but then arrest at the grain boundaries because these boundaries have higher tensile strength than the cleavage planes. Similarly, slices of the tomograms of the granite experiment show fractures that terminate at the edges of biotite grains (Figures 3c and 3d).

Tapponnier and Brace (1976) also observed the impeding influence of biotite relative to the surrounding quartz and feldspar in granite. In the field, fault propagation may also be modulated by heterogeneous strength distributions, such as foliated rock that produces well-defined directions of lower and higher strength (e.g., McBeck et al., 2017).

#### 4.3. Fracture Aperture

In addition to fracture length, fracture aperture is among the best predictors of fracture development in these experiments (Figure S6). Similar to the trend observed for fracture length, growing fractures tend to have smaller minimum eigenvalues than closing fractures (Figure 2B). These trends are consistent with analytical formulations of the stress intensity factor because thinner fractures are predicted to develop higher stress intensity factors than thicker fractures (Isida, 1971). In addition, sharper crack tips are predicted to develop higher stress intensity factors than rounded crack tips (Huang & Li, 2004). Thinner fractures may tend to have sharper tips than thicker fractures. The trend of thinner fractures growing, and thicker fractures closing may also arise from the ability of thicker fractures to close by larger volumes along their smallest dimension than thinner fractures.

#### 4.4. Fracture Orientation

Growing fractures tend to have more horizontal, perpendicular to  $\sigma_1$ , eigenvectors with the minimum eigenvalue than do closing fractures (Figure 2c). This trend may arise in part from the eigenvector with the maximum eigenvalue of fractures becoming more optimally oriented for sliding according to Mohr-Coulomb theory (Dahlen, 1984). Within the later stages of the monzonite experiment (100- to 150-MPa differential stress), the orientations of the long axis of the growing fractures match orientations that host the maximum Coulomb shear stress,  $\tau/\sigma_n$ , 30–60° from  $\sigma_1$ , while the short axes of the closing fractures become perpendicular to  $\sigma_1$  (Figure 2c).

### 5. Conclusions

Our analysis shows that growing fractures tend to be smaller in volume, shorter, thinner, more obliquely dipping from the main compressive stress direction, and more clustered, to at least one neighbor, than do closing fractures (Figure 4). Assuming that elastic interactions control the tendency for fractures to grow or close, we may cautiously extrapolate our results to crustal scales. Field analyses of crustal fault networks should focus on the length, orientation, and clustering of faults in order to robustly predict their likelihood of propagation. Such analyses may only need to consider the distance to the closest fault, rather than system-scale measures of clustering, for robust predictions of fault development.

### References

- Anderson, E. M. (1942). *The dynamics of faulting and dyke formation with applications to Britain*. Edinburgh and London: Oliver & Boyd. 15s
- Asencio-Cortés, G., Martínez-Álvarez, F., Troncoso, A., & Morales-Esteban, A. (2017). Medium-large earthquake magnitude prediction in Tokyo with artificial neural networks. *Neural Computing and Applications*, 28(5), 1043–1055. <https://doi.org/10.1007/s00521-015-2121-7>

#### Acknowledgments

We thank Elodie Boller, Paul Tafforeau, and Alexander Rack for providing advice on the design of the tomography setup and Sanchez Technology for building the deformation apparatus. Joachim Mathiesen, Paul Meakin, and Yehuda Ben-Zion provided suggestions on an early version of the manuscript that improved the study. The Norwegian Research Council funded this work (grant 272217). Beamtime was allocated at the European Synchrotron Radiation Facility (Long-Term Proposal ES-295). The Python scripts to build, train, and test the logistic regression models, and the corresponding experimental data, are available on GitHub ([https://github.com/jmbeck/Machine\\_Learning\\_Rock\\_Deformation](https://github.com/jmbeck/Machine_Learning_Rock_Deformation)). We thank Editor Lucy Flesch and two anonymous reviewers for suggestions that improved the manuscript.



- Asim, K. M., Martínez-Álvarez, F., Basit, A., & Iqbal, T. (2017). Earthquake magnitude prediction in Hindukush region using machine learning techniques. *Natural Hazards*, *85*(1), 471–486. <https://doi.org/10.1007/s11069-016-2579-3>
- Bergen, K. J., Johnson, P. A., Maarten, V., & Beroza, G. C. (2019). Machine learning for data-driven discovery in solid Earth geoscience. *Science*, *363*(6433). <https://doi.org/10.1126/science.aau0323>
- Bürgmann, R., Pollard, D. D., & Martel, S. J. (1994). Slip distributions on faults: Effects of stress gradients, inelastic deformation, heterogeneous host-rock stiffness, and fault interaction. *Journal of Structural Geology*, *16*(12), 1675–1690. [https://doi.org/10.1016/0191-8141\(94\)90134-1](https://doi.org/10.1016/0191-8141(94)90134-1)
- Cox, D. R. (1958). The regression analysis of binary sequences. *Journal of the Royal Statistical Society: Series B: Methodological*, *20*(2), 215–232.
- Dahlen, F. A. (1984). Noncohesive critical Coulomb wedges: An exact solution. *Journal of Geophysical Research*, *89*(B12), 10,125–10,133. <https://doi.org/10.1029/JB089iB12p10125>
- Griffith, A. A. (1921). VI. The phenomena of rupture and flow in solids. *Philosophical Transactions of the Royal Society of London. Series A, Containing Papers of a Mathematical or Physical Character*, *221*(582-593), 163–198.
- Guyon, I., Weston, J., Barnhill, S., & Vapnik, V. (2002). Gene selection for cancer classification using support vector machines. *Machine Learning*, *46*(1/3), 389–422. <https://doi.org/10.1023/A:1012487302797>
- Hosmer, D. W. Jr., Lemeshow, S., & Sturdivant, R. X. (2013). *Applied logistic regression* (Vol. 398). Hoboken, NJ: John Wiley & Sons.
- Huang, M., & Li, Z. (2004). Dislocation emission criterion from a blunt crack tip. *Journal of the Mechanics and Physics of Solids*, *52*(9), 1991–2003. <https://doi.org/10.1016/j.jmps.2004.03.003>
- Hubbert, M. (1951). Mechanical basis for certain familiar geologic structures. *Geological Society of America Bulletin*, *62*(4), 355–372. [https://doi.org/10.1130/0016-7606\(1951\)62\[355:MBFCFG\]2.0.CO;2](https://doi.org/10.1130/0016-7606(1951)62[355:MBFCFG]2.0.CO;2)
- Irwin, G. (1957). Analysis of stresses and strains near the end of a crack traversing a plate. *Journal of Applied Mechanics*, *24*, 361–364.
- Isida, M. (1971). Effect of width and length on stress intensity factors of internally cracked plates under various boundary conditions. *International Journal of Fracture Mechanics*, *7*(3), 301–316.
- Kandula, N., Cordonnier, B., Boller, E., Weiss, J., Dysthe, D. K., & Renard, F. (2019). Dynamics of microscale precursors establish brittle-compressive failure as a critical phenomenon in Carrara marble. *Journal of Geophysical Research: Solid Earth*, *124*, 6121–6139. <https://doi.org/10.1029/2019JB017381>
- McBeck, J., Cooke, M., & Madden, E. (2017). Work optimization predicts the evolution of extensional step overs within anisotropic host rock: Implications for the San Pablo Bay, CA. *Tectonics*, *36*, 2630–2646. <https://doi.org/10.1002/2017TC004782>
- Müller, A. C., & Guido, S. (2016). *Introduction to machine learning with Python: A guide for data scientists*. Sebastopol, CA: O'Reilly Media, Inc.
- Pedregosa, F., Varoquaux, G., Gramfort, A., Michel, V., Thirion, B., Grisel, O., et al. (2011). Scikit-learn: Machine learning in Python. *Journal of Machine Learning Research*, *12*(Oct), 2825–2830.
- Raju, I. S., & Newman, J. C. Jr. (1979). Stress-intensity factors for a wide range of semi-elliptical surface cracks in finite-thickness plates. *Engineering Fracture Mechanics*, *11*(4), 817–829. [https://doi.org/10.1016/0013-7944\(79\)90139-5](https://doi.org/10.1016/0013-7944(79)90139-5)
- Renard, F., Cordonnier, B., Dysthe, D. K., Boller, E., Tafforeau, P., & Rack, A. (2016). A deformation rig for synchrotron microtomography studies of geomaterials under conditions down to 10 km depth in the earth. *Journal of Synchrotron Radiation*, *23*(4), 1030–1034. <https://doi.org/10.1107/S1600577516008730>
- Renard, F., Cordonnier, B., Kobchenko, M., Kandula, N., Weiss, J., & Zhu, W. (2017). Microscale characterization of rupture nucleation unravels precursors to faulting in rocks. *Earth and Planetary Science Letters*, *476*, 69–78. <https://doi.org/10.1016/j.epsl.2017.08.002>
- Renard, F., Weiss, J., Mathiesen, J., Ben-Zion, Y., Kandula, N., & Cordonnier, B. (2018). Critical evolution of damage toward system-size failure in crystalline rock. *Journal of Geophysical Research: Solid Earth*, *123*, 1969–1986. <https://doi.org/10.1002/2017JB014964>
- Reyes, J., Morales-Esteban, A., & Martínez-Álvarez, F. (2013). Neural networks to predict earthquakes in Chile. *Applied Soft Computing*, *13*(2), 1314–1328. <https://doi.org/10.1016/j.asoc.2012.10.014>
- Rouet-Leduc, B., Hulbert, C., Lubbers, N., Barros, K., Humphreys, C. J., & Johnson, P. A. (2017). Machine learning predicts laboratory earthquakes. *Geophysical Research Letters*, *44*, 9276–9282. <https://doi.org/10.1002/2017GL074677>
- Rybicki, E. F., & Kanninen, M. F. (1977). A finite element calculation of stress intensity factors by a modified crack closure integral. *Engineering Fracture Mechanics*, *9*(4), 931–938. [https://doi.org/10.1016/0013-7944\(77\)90013-3](https://doi.org/10.1016/0013-7944(77)90013-3)
- Sih, G. C. (1974). Strain-energy-density factor applied to mixed mode crack problems. *International Journal of Fracture*, *10*(3), 305–321. <https://doi.org/10.1007/BF00035493>
- Tapponnier, P., & Brace, W. F. (1976). Development of stress-induced microcracks in Westerly granite. In *International Journal of Rock Mechanics and Mining Sciences & Geomechanics Abstracts* (Vol. 13, No. 4, pp. 103–112). Pergamon: Pergamon Press.
- Wesnowsky, S. G. (2006). Predicting the endpoints of earthquake ruptures. *Nature*, *444*(7117), 358–360. <https://doi.org/10.1038/nature05275>